

# PCCP

Accepted Manuscript



This is an *Accepted Manuscript*, which has been through the Royal Society of Chemistry peer review process and has been accepted for publication.

*Accepted Manuscripts* are published online shortly after acceptance, before technical editing, formatting and proof reading. Using this free service, authors can make their results available to the community, in citable form, before we publish the edited article. We will replace this *Accepted Manuscript* with the edited and formatted *Advance Article* as soon as it is available.

You can find more information about *Accepted Manuscripts* in the [Information for Authors](#).

Please note that technical editing may introduce minor changes to the text and/or graphics, which may alter content. The journal's standard [Terms & Conditions](#) and the [Ethical guidelines](#) still apply. In no event shall the Royal Society of Chemistry be held responsible for any errors or omissions in this *Accepted Manuscript* or any consequences arising from the use of any information it contains.

Cite this: DOI: 10.1039/c0xx00000x

ARTICLE TYPE

www.rsc.org/xxxxxx

Theoretical Study of  $\Delta^3$ -(+)-Carene OxidationLeonardo Baptista\*<sup>a</sup>, Lilian Fernandes<sup>a</sup>, Jacques Fernandes Dias<sup>a</sup>, Edilson Clemente da Silva<sup>b</sup>, Claudio Vinicius Ferreira dos Santos<sup>b</sup>, Felipe Simões Gil de Mendonça<sup>b</sup>, Graciela Arbilla<sup>c</sup>

Received (in XXX, XXX) Xth XXXXXXXXXX 20XX, Accepted Xth XXXXXXXXXX 20XX

DOI: 10.1039/b000000x

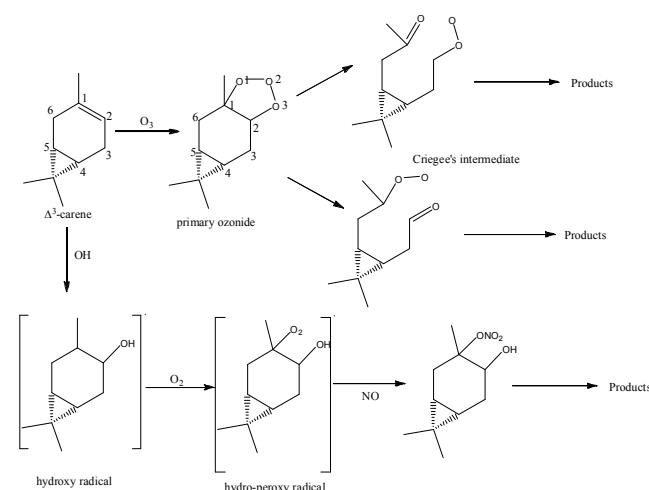
In this work, the rate-limiting steps of  $\Delta^3$ -carene oxidation by ozone and OH radicals were studied. The thermochemical and kinetic parameters were evaluated using the B3LYP, PBE1PBE and BHandHLYP functionals, coupled cluster methods and the 6-311G(d,p) and 6-311++G(d,p) basis sets. The attack on the double bond may occur in different orientations, leading to different oxidation products. The rate coefficients of each step of the reactions were evaluated using conventional canonical transition-state theory and variational canonical transition-state theory whenever necessary. The theoretical rate coefficient for the ozonolysis mechanism, evaluated at the CCSD(T)/6-31G(d,p)//PBE1PBE/6-311++G(d,p) level, was  $2.08 \times 10^{-17} \text{ cm}^3 \text{ molecule}^{-1} \text{ s}^{-1}$ . The coefficient for the oxidation initialised by the OH radical, calculated at the BHandHLYP/6-311++G(d,p) level, was  $5.06 \times 10^{-12} \text{ cm}^3 \text{ molecule}^{-1} \text{ s}^{-1}$ . These values are in reasonable agreement with the experimental results. The importance of these reactions in atmospheric chemistry is discussed.

## Introduction

The oxidation of volatile organic compounds (VOCs) in the atmosphere plays an important role in tropospheric chemistry. The oxidation of hydrocarbons leads to ozone formation and photochemical smog phenomena.<sup>1</sup> The scientific community agrees that oxidation products can affect the health of the population, the climate, and secondary organic aerosol (SOA) formation.<sup>2,3,4,5</sup> Much effort has been devoted to studying the gas-phase oxidation of terpenes emitted into the atmosphere to describe the influence of their oxidation products on SOA formation.<sup>2,3,4,6,7,8</sup>

Terpenes are the VOCs most profusely emitted by biogenic sources,<sup>3</sup> mainly plants. Their structures are constructed from isoprenoid units, which may lead to monoterpenes (C<sub>10</sub>), sesquiterpenes (C<sub>15</sub>), diterpenes (C<sub>20</sub>), and triterpenes (C<sub>30</sub>) in the biosynthetic pathway.<sup>9</sup> In the atmosphere, terpenes exhibit alkene-like chemistry because of the presence of double bonds in their structures, thus resulting in the addition of ozone or OH radicals to these unsaturated systems. These reactions constitute the major sinks of terpenes in the troposphere.<sup>6,10</sup>

The accepted ozonolysis mechanism follows Criegee's proposal, in which ozone adds to a double bond to form a primary ozonide (POZ). The resulting POZs are vibrationally excited and readily decompose, forming two new species: a Criegee intermediate (CI) and a primary carbonyl.<sup>7,11,12,13,14</sup> (Figure 1). The most recent theoretical studies report the electronic structure of the CI to be

zwitterionic.<sup>15,16</sup>

**Fig. 1** First steps for  $\Delta^3$ -carene oxidation in the atmosphere. Reactions initiated by ozone and an OH radical.

After ozone addition to the double bonds, the products may decompose by several unimolecular reactions or react with atmospheric gases. Alternatively, OH radical addition leads to the formation of hydroxyalkyl radicals, which rapidly react with O<sub>2</sub> to form hydroxyalkyl peroxy radicals, which, in turn, react with NO, NO<sub>2</sub>, HO<sub>2</sub> and organic peroxy radicals (and, presumably, the NO<sub>3</sub> radical) (Figure 1). In addition to the major OH radical addition pathway, the hydrogen abstraction of allylic hydrogen

also occurs as a minor process.<sup>17</sup> The OH radical is the second most powerful oxidant (just after molecular fluorine - F<sub>2</sub>) and therefore the study of its reactivity with natural compounds in our atmosphere is of great importance, even if its life-time is very short. In both oxidation mechanisms, the final products are extremely dependent on the pollutants present in the atmosphere and on humidity.<sup>1,5,18,19</sup>

Several theoretical studies of the oxidation of isoprene and other terpenes have been reported in the literature. These studies were focused on certain well-known species observed in the atmosphere, e.g.,  $\alpha$ - and  $\beta$ -pinene, limonene, geraniol, and citronellol. However, to our knowledge, no theoretical studies to date have evaluated the kinetic parameters for  $\Delta^3$ -carene oxidation. The  $\Delta^3$ -carene (3,7,7-trimethylbicyclo[4.1.0]hept-3-ene) is emitted by trees of the genus *Pinus*, which are found in coniferous forests.<sup>20</sup> This species of trees is used in the manufacture of pellets, briquettes, and paper, which has prompted certain industries to create artificial forests to satisfy their wood demands. In addition,  $\Delta^3$ -carene and its oxidation products have been found in SOAs.<sup>3,21</sup> To date, only chamber and kinetic modelling studies have been performed to identify the oxidation products,<sup>22</sup> examine the temporal behaviour of reactants, and determine the rate coefficients for  $\Delta^3$ -carene oxidation. Colville and Griffin<sup>23</sup> used the protocol developed by Jenkin<sup>24</sup> and the structural similarities between pinene and carene in their mechanistic study because of the lack of specific information concerning the reaction paths in  $\Delta^3$ -carene oxidation.

The main goal of this study is to evaluate the kinetic parameters for  $\Delta^3$ -carene oxidation through reaction with O<sub>3</sub> and OH radicals. The discussion will focus primarily on the rate-limiting step of these reactions: the addition of oxidants to the double bond.

## Computational Details

The geometries of all species that are part of the reaction mechanism were completely optimised without any geometry constraints. The structures were classified as minima or saddle points of the potential-energy surface by the analysis of harmonic vibrational frequencies. The density functional methods B3LYP, BHandHLYP, and PBE1PBE were used for geometry optimisations and frequency calculations. Two basis sets were employed: 6-311G(d,p) and 6-311++G(d,p). The thermochemical and kinetic parameters were provided by single-point energy evaluations using the coupled-cluster method. For OH radical addition, single-point energy calculations were performed at the CCSD/6-31G(d,p) level by considering the BHandHLYP/6-311G(d,p) geometry (i.e., at the CCSD/6-31G(d,p)//BHandHLYP/6-311G(d,p) level). For the ozonolysis mechanism, the electronic energy was corrected at the CCSD/6-31G(d,p) and CCSD(T)/6-31G(d,p) levels considering the PBE1PBE/6-311++G(d,p) geometry (i.e., at the CCSD/6-31G(d,p)//PBE1PBE/6-311++G(d,p) and CCSD(T)/6-31G(d,p)//PBE1PBE/6-311++G(d,p) levels).

The kinetic parameters were evaluated using the canonical transition-state theory (TST) equation (equation 1):

$$k(T) = \frac{k_b T}{h} e^{-\frac{\Delta G^\ddagger}{RT}} \quad (1)$$

where  $h$  is Planck's constant,  $T$  is the temperature,  $k_b$  is Boltzmann's constant,  $\Delta G^\ddagger$  is the free energy of activation of each reaction step, and  $R$  is the universal gas constant. The initial steps of olefin oxidation—the addition of ozone or OH radical—are the rate-limiting steps of this mechanism.<sup>17</sup> The theoretical rate coefficient evaluated for the formation of primary ozonides and hydroxyl radicals may then be compared directly to the experimental rate coefficients.

All the quantum chemical calculations were performed using the Gaussian 03 and Orca 2.9 software packages.<sup>25,26</sup> Certain aspects of the reaction mechanism were analysed by numerical integration of the rate equations using the theoretical rate coefficients evaluated in this work. Kintecus version 4.55 was used to integrate the rate equations.<sup>27</sup>

## Results and Discussion

The optimised geometry of  $\Delta^3$ -carene and the orientations where the OH radical and ozone may attack are shown in Figure 2. The highlighted portion of the structure is the endocyclic double bond. Because of the lack of symmetry, two different primary ozonides and four products of OH radical addition are expected. Each mechanism will be discussed in a different section, and their implications on atmospheric chemistry will be analysed in the final section.

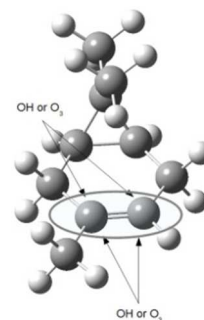


**Fig. 2** Optimised geometry of  $\Delta^3$ -carene at the BHandHLYP/6-311++G(d,p) level. The highlighted part shows the sites available for ozone and OH-radical addition.

### Ozonolysis Reaction

Ozonolysis reactions are generally accepted to follow the well-known Criegee mechanism: (1) ozone is added to a double bond to form a primary ozonide; (2) the ozonide is formed in a highly exothermic reaction and breaks apart into a carbonyl compound and a Criegee intermediate (CI); and (3) the CI in the gas phase decomposes mainly via unimolecular reactions. As expected, the results obtained in this work show that this behaviour is also observed for the reaction of  $\Delta^3$ -carene with ozone. Table 1 lists key geometric parameters for the transition structures and POZs, and Figure 3 contains the free energies of activation and reaction for ozone addition to the double bond. The two transition structures are labelled TS<sub>top</sub> and TS<sub>bottom</sub>.

The results given in Table 1 show that changing the double bond to a single bond is characterised by an increase in the rC1C2 bond distance of approximately 18%. The average rC1C2 bond distance found in both ozonides is 1.56 Å, whereas the average distance in  $\Delta^3$ -carene is 1.32 Å. The most significant geometric parameters of both ozonides and transition structures (TSs) are

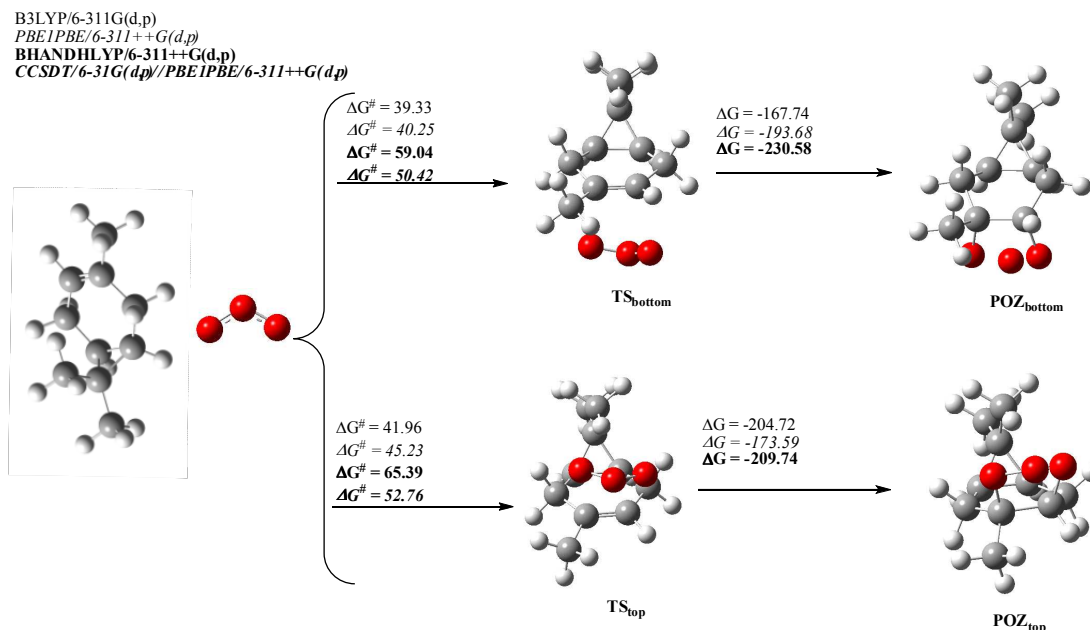


**Fig. 3** Free energies of activation and reaction for ozone addition to the  $\Delta^3$ -carene's double bond, calculated at four different levels. All values are in  $\text{kJ mol}^{-1}$ .

**Table 1** Geometric parameters for ozone addition to the double bond. Bond distances are shown in angstroms, bond and dihedral angles in degrees. The atom numbering is described in Figure 1.

	TS <sub>top</sub>	POZ <sub>top</sub>	TS <sub>bottom</sub>	POZ <sub>bottom</sub>
PBE1PBE/6-311++G(d,p)				
rC <sub>1</sub> O <sub>1</sub>	2.373	1.440	2.293	1.439
rC <sub>2</sub> O <sub>3</sub>	2.335	1.426	2.254	1.425
rC <sub>1</sub> C <sub>2</sub>	1.372	1.567	1.377	1.563
∠C <sub>1</sub> O <sub>1</sub> O <sub>2</sub>	97.15	103.20	100.29	104.12
∠C <sub>1</sub> O <sub>1</sub> O <sub>2</sub> O <sub>3</sub>	62.32	51.07	49.24	47.65
BHandHLYP/6-311++G(d,p)				
rC <sub>1</sub> O <sub>1</sub>	2.301	1.434	2.285	1.434
rC <sub>2</sub> O <sub>3</sub>	2.277	1.421	2.237	1.421
rC <sub>1</sub> C <sub>2</sub>	1.368	1.561	1.369	1.561
∠C <sub>1</sub> O <sub>1</sub> O <sub>2</sub>	97.96	103.83	100.31	103.83
∠C <sub>1</sub> O <sub>1</sub> O <sub>2</sub> O <sub>3</sub>	61.64	49.98	50.86	49.98

similar; the major difference is the orientation of ozone addition to the double bond. The effect of steric hindrance may be responsible for the slight difference in the rC<sub>2</sub>O<sub>1</sub> and rC<sub>2</sub>O<sub>3</sub> bond distances between TS<sub>top</sub> and TS<sub>bottom</sub>. The bond distances in TS<sub>top</sub> are longer (rC<sub>2</sub>O<sub>1</sub> is 0.080 Å longer and rC<sub>2</sub>O<sub>3</sub> is 0.081 Å longer), most likely because of repulsions between ozone and the bicyclic group.

In certain studies, a pre-barrier complex, stabilised by a few  $\text{kJ mol}^{-1}$  in relation to the isolated reactants, has been proposed.<sup>28,29,30</sup> This species would be responsible for additional stabilisation of the reactants, thus justifying the negative values observed for critical energies in this type of reaction. The present results agree with those of the previous study by Oliveira and Bauerfeldt,<sup>28</sup> who pointed out that negative values of the critical energies are dependent on the basis set. Table 2 lists the critical values evaluated at different levels and illustrates the basis-set

effect. For example, the inclusion of diffuse functions in the PBE1PBE functional leads to negative values for  $E^0$ , whereas the BHandHLYP functional is less affected by the addition of diffuse functions. Considering these effects, the authors found it more meaningful to describe and discuss the addition to double bonds in terms of Gibbs free energies.

As expected, all methods predict that the reactions forming ozonides are highly exoergic,  $\Delta G < -167 \text{ kJ mol}^{-1}$ . Addition to the double bond on the side with lower steric hindrance (bottom attack) is favoured by approximately  $4.19 \text{ kJ mol}^{-1}$  with respect to free energy of activation. The major contributor to  $\Delta G^\ddagger$  is the entropic effects. By analysing the bottom attack at the PBE1PBE/6-311++G(d,p) level, we determined the enthalpy of activation to be  $-10.08 \text{ kJ mol}^{-1}$  and the entropic contribution to activation free energy ( $T\Delta S^\ddagger$ ) to be, at 298 K,  $-50.33 \text{ kJ mol}^{-1}$ . This pattern was observed for all methods and has been noted previously in other ozonolysis studies.<sup>31</sup>

**Table 2** Critical energies evaluated at different levels for the ozonolysis reaction of  $\Delta^3$ -carene. All values are in  $\text{kJ mol}^{-1}$ .

	TS <sub>top</sub>	TS <sub>bottom</sub>
B3LYP/6-311G(d,p)	-6.94	-7.07
BHandHLYP/6-311G(d,p)	8.87	9.66
BHandHLYP/6-311++G(d,p)	12.59	16.11
PBE1PBE/6-311G(d,p)	11.59	12.30
PBE1PBE/6-311++G(d,p)	-7.99	-4.77

The rate coefficients evaluated for ozonide formation by conventional transition-state theory, using the activation Gibbs free energy presented in Figure 3, are listed in Table 3. The branching ratio calculated for ozone addition predicts that more than 80% of the yield will occur in the bottom orientation, as expected, because of high steric hindrance in the top orientation. The best agreement with the reported experimental overall

**Table 3** Rate coefficient for each  $\Delta^3$ -carene ozonolysis channel and the overall rate coefficient ( $k_{\text{total}} = k_{\text{top}} + k_{\text{bottom}}$ ) at 298 K. The bimolecular rate coefficients are in  $\text{cm}^3 \text{ molecule}^{-1} \text{ s}^{-1}$ . The branching ratios for each channel are stated in parentheses.

Method	POZ <sub>top</sub>	POZ <sub>bottom</sub>	Total
		TST	
B3LYP/6-311G(d,p)	$4.0 \times 10^{-16}$ (0.25)	$1.2 \times 10^{-15}$ (0.75)	$1.6 \times 10^{-15}$
PBE1PBE/6-311G(d,p)	$1.57 \times 10^{-19}$ (0.16)	$8.14 \times 10^{-19}$ (0.84)	$9.71 \times 10^{-19}$
BHandHLYP/6-311G(d,p)	$1.58 \times 10^{-19}$ (0.18)	$7.15 \times 10^{-19}$ (0.82)	$8.73 \times 10^{-19}$
PBE1PBE/6-311++G(d,p)	$1.1 \times 10^{-16}$ (0.12)	$8.0 \times 10^{-16}$ (0.88)	$9.0 \times 10^{-16}$
BHandHLYP/6-311++G(d,p)	$3.15 \times 10^{-20}$ (0.07)	$4.06 \times 10^{-19}$ (0.93)	$4.4 \times 10^{-19}$
CCSD/6-31G(d,p)//PBE1PBE/6-311++G(d,p)	$1.51 \times 10^{-20}$ (0.27)	$4.09 \times 10^{-20}$ (0.73)	$5.60 \times 10^{-20}$
CCSD/6-311G(d,p)//PBE1PBE/6-311++G(d,p)	$6.08 \times 10^{-21}$ (0.37)	$1.05 \times 10^{-20}$ (0.63)	$1.66 \times 10^{-20}$
CCSD(T)/6-31G(d,p)//PBE1PBE/6-311++G(d,p)	$5.86 \times 10^{-18}$ (0.28)	$1.50 \times 10^{-17}$ (0.72)	$2.08 \times 10^{-17}$
Experimental <sup>a</sup>			$3.8 \times 10^{-17} \pm 4.1 \times 10^{-18}$
			$1.0 \times 10^{-16}$
			$5.9 \times 10^{-17} \pm 1.0 \times 10^{-17}$

<sup>a</sup> References <sup>32a,b,c</sup>, respectively

coefficients was obtained at PBE1PBE/6-311++G(d,p),  $k(T) = 9.0 \times 10^{-16} \text{ cm}^3 \text{ molecule}^{-1} \text{ s}^{-1}$ . The improved calculated value differs from the experimental coefficients by less than one order of magnitude.

The structure of  $\Delta^3$ -carene resembles that of  $\alpha$ -pinene, as reflected in the rate coefficients for the ozonolysis processes, with the same magnitude. The reported rates for  $\alpha$ -pinene are in the range of  $0.28 \times 10^{-16}$  to  $3.3 \times 10^{-16} \text{ cm}^3 \text{ molecule}^{-1} \text{ s}^{-1}$ ,<sup>33,34,35,36,37,38</sup> in agreement with the experimental and theoretical values for  $\Delta^3$ -carene. When the bicyclic terpene possesses an exocyclic double bond, the rate coefficients tend to be lower:  $1.2 \times 10^{-17}$  to  $6.5 \times 10^{-17} \text{ cm}^3 \text{ molecule}^{-1} \text{ s}^{-1}$  for the ozonolysis of  $\beta$ -pinene<sup>33,34,35,36,37,38</sup> and  $4.5 \times 10^{-19}$  to  $9.0 \times 10^{-19} \text{ cm}^3 \text{ molecule}^{-1} \text{ s}^{-1}$  for camphene ozonolysis.<sup>39,40</sup> However, the evaluation of the Arrhenius parameters remains a challenge to the predictive power of DFT methods. Despite the reasonable agreement between the calculated rate coefficients at the PBE1PBE/6-311++G(d,p) level and the experimental values, the Arrhenius equation shows an unexpected slight negative dependence on temperature. This negative dependence is related to the negative value of the critical energy for ozone addition, which is probably associated with basis-set effects. Previous ozonolysis studies have shown that this type of reaction exhibits a small positive dependence on the temperature,<sup>28,31a,37</sup> suggesting that the profile obtained with the PBE1PBE functional is attributable to the basis set. The similarity between the carene and pinene structures reinforces the expectation of a positive dependence of the rate coefficient on temperature. An exception found in the relevant literature is the Arrhenius equation obtained by Nguyen *et al.*<sup>41</sup> for  $\beta$ -caryophyllene ozonolysis, which shows a small negative dependence on temperature. The authors concluded that this ozonolysis reaction has no barrier and that  $k(T)$  can be considered nearly constant over all the relevant atmospheric conditions. However, no experimental information or other theoretical results exist to compare with Nguyen's results and verify whether the

profile obtained is due to the methodology or is a system feature. The negative dependence observed in the Arrhenius equation may also be related to the existence of a pre-reactive complex in the potential energy surface; such a structure has been characterised theoretically for other terpenoids.<sup>42</sup>

The electronic energy was corrected at the CCSD/6-31G(d,p), CCSD/6-311G(d,p), and CCSD(T)/6-31G(d,p) levels considering the PBE1PBE/6-311++G(d,p) geometry and vibrational corrections to improve the theoretical rate coefficient and Arrhenius parameters. The results obtained using these methods are shown in Table 3. Using the barriers calculated at the CCSD(T)/6-31G(d,p)//PBE1PBE/6-311++G(d,p) level, a global rate coefficient of  $2.08 \times 10^{-17} \text{ cm}^3 \text{ molecule}^{-1} \text{ s}^{-1}$  was obtained, in good agreement with the experimental rate coefficients measured at 295 and 296 K. The expected positive dependence upon temperature is also observed, as shown in Figure 4. The theoretical modified Arrhenius expressions are shown in Equations 2, 3 and 4. From these expressions, we concluded that because of the small temperature influence on the rate coefficient and the pre-exponential factor, the rate coefficient for carene ozonolysis can be considered constant for most atmospheric chemistry purposes.

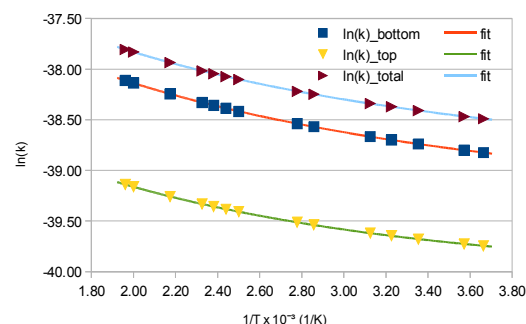


**Fig. 4** Plots of theoretical values of  $\ln(k)$  vs.  $T^{-1}$ . The fitted curves were obtained using the generalised Arrhenius expression. The rate coefficients were evaluated using the TST equation and  $\Delta G^\ddagger$  evaluated at the CCSD(T)/6-31G(d,p)//PBE1PBE/6-311++G(d,p) level.

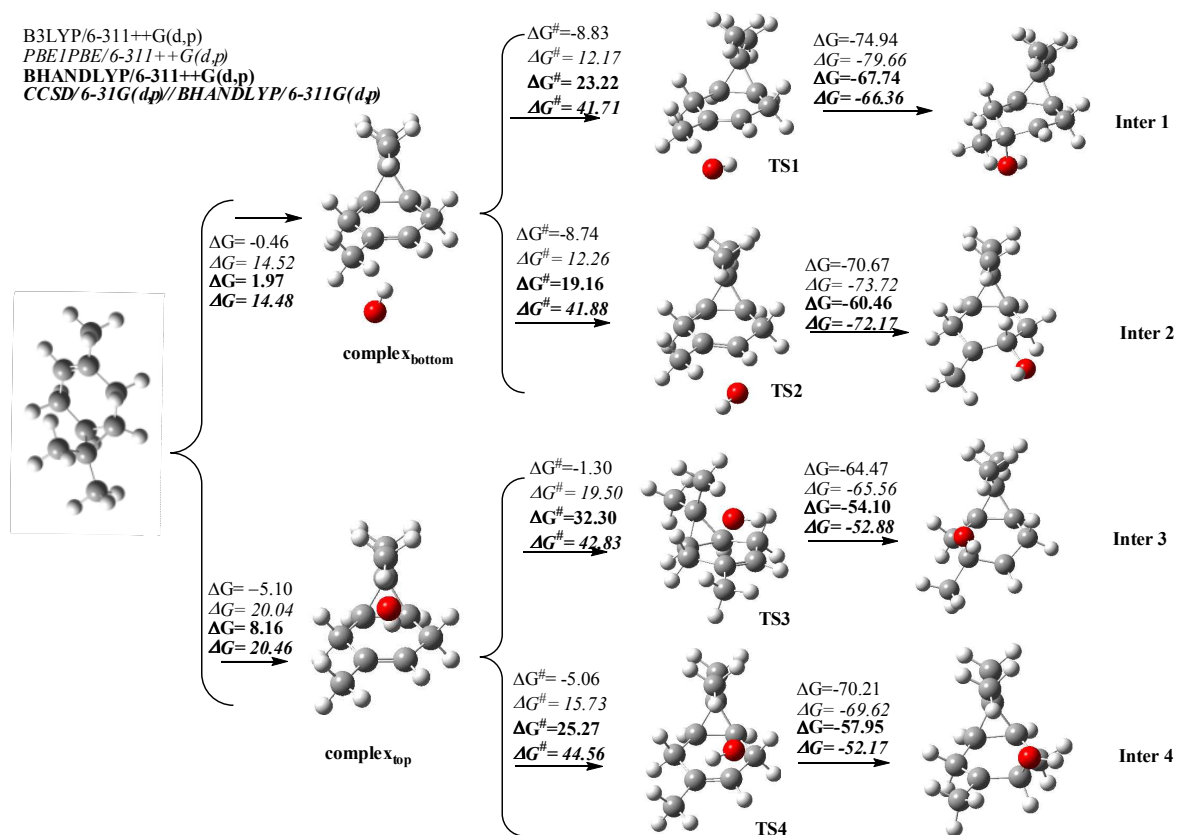


Fig. 5 Free energies of activation and reaction for OH radical addition to the  $\Delta^3$ -carene double bond. All values are in  $\text{kJ mol}^{-1}$ .

5

Table 4 Geometric parameters for OH radical addition to the  $\Delta^3$ -carene double bond. Bond distances are in angstroms. Bond and dihedral angles are in degrees.

	TS1	Inter1	TS2	Inter2	TS3	Inter3	TS4	Inter4
PBE1PBE/6-311++G(d,p)								
rCO	2.308	1.444	2.284	1.423	2.434	1.453	2.224	1.444
rC <sub>1</sub> C <sub>2</sub>	1.355	1.495	1.356	1.495	1.357	1.491	1.361	1.489
$\theta$ CCO	77.47	109.36	79.13	113.56	68.26	105.76	90.42	106.90
$\psi$ CCOH	-77.37	-65.82	73.91	-71.68	114.92	-177.60	63.48	172.07
BHandHLYP/6-311++G(d,p)								
rCO	2.098	1.437	2.129	1.418	2.100	1.444	2.134	1.436
rC <sub>1</sub> C <sub>2</sub>	1.359	1.530	1.354	1.496	1.361	1.491	1.354	1.489
$\theta$ CCO	91.82	109.14	94.39	113.20	91.20	108.88	95.53	106.93
$\psi$ CCOH	-50.38	55.36	101.84	-73.11	-50.71	-57.94	56.44	171.07

$$k_{bottom}(T) = 3.33 \times 10^{-22} \times T^{1.74} e^{\frac{224.03(K)}{T}} \text{ cm}^3 \text{ molec}^{-1} \text{ s}^{-1} \quad (2)$$

$$k_{top}(T) = 1.30 \times 10^{-22} \times T^{1.72} e^{\frac{275.33(K)}{T}} \text{ cm}^3 \text{ molec}^{-1} \text{ s}^{-1} \quad (3)$$

$$k_{total}(T) = 4.45 \times 10^{-22} \times T^{1.75} e^{\frac{240.01(K)}{T}} \text{ cm}^3 \text{ molec}^{-1} \text{ s}^{-1} \quad (4)$$

Considering the energetic data computed at the CCSD(T)/6-31G(d,p)/PBE1PBE/6-311++G(d,p) level, the Arrhenius equation has a slight negative theoretical activation energy for the overall ozonolysis reaction. This fact, which was observed in all addition channels, indicates that entropy provides the major contribution to the energy barrier for ozonolysis. The results in

this study indicate the importance of including the triple excitations in the coupled cluster method to improve the evaluation of the ozonolysis rate coefficient.

### Oxidation by OH radical

The OH radical attack on the double bond proceeds as follows: (a) OH approaches  $\Delta^3$ -carene, leading to a radical dipole pre-complex; (b) the pre-complex rearranges to form a carbon-oxygen bond; (c) a new free radical is formed, ready to react with atmospheric gases. According to the literature, the abstraction of allylic hydrogen is, in most cases, a minor pathway of oxidation (in general, it represents less than 10%).<sup>43,44,45</sup> However, certain exceptions have been observed, such as for  $\alpha$ -phellandrene,  $\alpha$ -

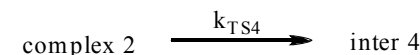
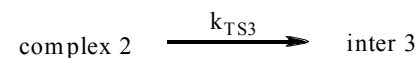
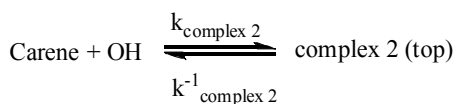
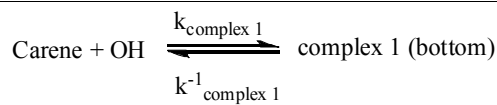
terpinene,<sup>46</sup> citronellol<sup>47</sup> and  $\alpha$ -terpineol.<sup>48</sup> Hydrogen abstraction contributes with  $30 \pm 7\%$  for  $\alpha$ -terpinene's oxidation and  $27 \pm 10\%$  for  $\alpha$ -phellandrene's oxidation.<sup>46</sup> For  $\alpha$ -terpineol, the 4-methyl-3-cyclohexen-1-one is the main product formed by

hydrogen abstraction of the unsaturated tertiary carbon on the terpineol cycle.<sup>48</sup> Citronellol presents two abstraction distinct sites that contributes with nearly 7% to the overall oxidation mechanism and the products related to this mechanism were measured.<sup>47,49</sup>

Two different pre-complex structures were found; they are labelled as  $\text{complex}_{\text{top}}$  and  $\text{complex}_{\text{bottom}}$  in Figure 5. In these structures, the hydrogen in the OH radical interacts with the double bond. The OH rotates to provide the correct orientation to form the carbon-oxygen bond. Four different transition structures, labelled TS1, TS2, TS3, and TS4, were optimised, and their connectivity with the reactants and products was confirmed by evaluation of the intrinsic reaction coordinate (Supplementary Material Section). For the transition structures, the rCO bond distances are approximately 2.3 Å, and longer distances were observed for the top orientation because of the repulsion between the OH radical and the dimethyl groups in  $\Delta^3$ -carene (Table 4). After the addition of the OH radical, the rCO bond distances are equal to the average value for a carbon-oxygen single bond, i.e., approximately 1.4 Å.

Figure 5 shows the thermochemistry of OH radical addition to the  $\Delta^3$ -carene double bond at the four different addition sites. All possible reactions are exoergic, with  $\Delta G$  values as high as  $-332.63 \text{ kJ mol}^{-1}$ ; the lowest values were obtained at the CCSD/6-31G\*\*//BHandHLYP/6-311G\*\* level. A steric hindrance effect is observed for the addition in the top orientation. The  $\Delta G^\ddagger$  values presented in Figure 5 show that this parameter increases by approximately  $35.14 \text{ kJ mol}^{-1}$  in the top orientation compared with the bottom orientation.

The calculation of kinetic parameters may include the formation and decomposition of the radical-dipole complexes obtained for this mechanism. The effect of radical-dipole complexes on the kinetics of OH radical addition to double bonds is well documented in the literature.<sup>43,50</sup> The negative dependence of  $k(T)$  on temperature is related to the existence of pre-barrier complexes (two complexes in this case) in conjunction with a transition structure with an electronic energy lower than those of the separated reactants. As suggested in the literature, the OH addition involves the formation of an intermediate—a pre-barrier complex—stabilised by a few  $\text{kJ mol}^{-1}$  in relation to the isolated reactants. The saddle point for the conversion of the pre-barrier complex to the intermediate products is located above the intermediate but below the isolated reactants, leading to non-Arrhenius behaviour with negative overall activation energies. Further, the pre-barrier complex (radical-dipole complex) can decompose either directly to intermediates or back to reactants. By considering all processes and the four possible reaction channels, we can express the overall rate coefficient by considering the following mechanism:



$$\frac{d[\text{carene}]}{[\text{OH}]} = - \left( k_{\text{complex 1}} \left( \frac{k_{\text{TS1}} + k_{\text{TS2}}}{k_{\text{complex 1}}^{-1} + k_{\text{TS1}} + k_{\text{TS2}}} \right) + k_{\text{complex 2}} \left( \frac{k_{\text{TS3}} + k_{\text{TS4}}}{k_{\text{complex 2}}^{-1} + k_{\text{TS3}} + k_{\text{TS4}}} \right) \right) [\text{carene}][\text{OH}] \quad (5)$$

where  $k_{\text{TS}}$  is the rate coefficient for radical-dipole complex decomposition in hydroxyl radicals,  $k_{\text{complex}}$  the rate coefficient for the formation of complexes by reactants, and  $k_{\text{complex}}^{-1}$  is the rate coefficient for the decomposition of complexes back to reactants. The two terms in parentheses represent each oxidation addition channel. The expression was obtained by considering the steady state approach for both complexes and by assuming that intermediates cannot return to radical-dipole complexes.<sup>43,51</sup>

The rate coefficients  $k_{\text{TS1}}$ ,  $k_{\text{TS2}}$ ,  $k_{\text{TS3}}$ , and  $k_{\text{TS4}}$  were evaluated by the optimisation of saddle points on the potential energy surface and by applying the TST equation at 298 K. The formation of pre-reactive complexes does not show a saddle point, thus requiring a variational evaluation of the rate coefficient. In this case, the rCO bond distance in both complexes was stretched and the Gibbs free energy was maximised along the dissociation pathway. The maximum value of the free energy was used in the TST equation to estimate the variational coefficient. These results are given in Table 5. Because of the computational cost of the variational approach, the rate coefficients were evaluated only at the BHandHLYP/6-311G(d,p) and BHandHLYP/6-311++G(d,p) levels. The theoretical overall rate coefficient, considering the higher basis, was calculated to be  $2.2 \times 10^{-12} \text{ cm}^3 \text{ molecule}^{-1} \text{ s}^{-1}$ , which is in reasonable agreement with the experimental value of  $8.7 \times 10^{-11} \text{ cm}^3 \text{ molecule}^{-1} \text{ s}^{-1}$ . The inclusion of diffuse functions in the basis set appears to be very important, as the overall rate coefficient evaluated using the 6-311++G(d,p) basis set is  $1.0 \times 10^{-14} \text{ cm}^3 \text{ molecule}^{-1} \text{ s}^{-1}$ .

The overall rate coefficient was evaluated following the approach of Colville and Griffin,<sup>23</sup> where the abstraction channel accounts for less than 10% of the overall mechanism. To test this approach, the abstraction of two allylic hydrogens (at carbons 3 and 6) was evaluated at the BHandHLYP/6-311G(d,p) and

BHandHLYP/6-311++G(d,p) levels. In these calculations, only the abstraction on the side with less steric hindrance was considered (Figure 6). The transition structures present the hydrogen at an intermediate distance between the carbon atom and the oxygen atom. At the BHandHLYP/6-311++G(d,p) level, the rate coefficient for hydrogen abstraction on carbon 3 is  $1.87 \times 10^{-12} \text{ cm}^3 \text{ molecule}^{-1} \text{ s}^{-1}$  and is  $9.84 \times 10^{-13} \text{ cm}^3 \text{ molecule}^{-1} \text{ s}^{-1}$  for hydrogen abstraction on carbon 6. These rate coefficient values indicate that the abstraction channels should be important in  $\Delta^3$ -carene oxidation. The abstraction reaction is included in the overall rate coefficient by summing the value obtained with

**Table 5** Rate coefficient for each channel of OH radical addition at 298 K and overall rate coefficient at the BHandHLYP/6-311++G(d,p) level. Unimolecular rate coefficients are presented in units of  $\text{s}^{-1}$  and bimolecular rate coefficients in  $\text{cm}^3 \text{ molecule}^{-1} \text{ s}^{-1}$ .

Rate coefficient	Value
$k_{\text{complex\_bottom}}$	$2.2 \times 10^{-11}$
$k^{-1}_{\text{complex\_bottom}}$	$2.7 \times 10^{+10}$
$k_{\text{complex\_top}}$	$1.29 \times 10^{-11}$
$k^{-1}_{\text{complex\_top}}$	$2.1 \times 10^{+11}$
$k_{\text{TS1}}$	$5.4 \times 10^{+8}$
$k_{\text{TS2}}$	$2.7 \times 10^{+9}$
$k_{\text{TS3}}$	$1.4 \times 10^{+7}$
$k_{\text{TS4}}$	$2.3 \times 10^{+8}$
$k_{\text{abs}}(\text{C3})$	$1.87 \times 10^{-12}$
$k_{\text{abs}}(\text{C6})$	$9.84 \times 10^{-13}$
$k_{\text{overall}}$ (only addition)	$2.2 \times 10^{-12}$
$k_{\text{overall}}$ (addition plus abstraction)	$5.06 \times 10^{-12}$
Experimental <sup>52a</sup>	$8.7 \times 10^{-11}$
Experimental <sup>52b</sup>	$8.51 \times 10^{-11}$
Evaluated theoretically by structure-reactivity relationships <sup>52c</sup>	$9.1 \times 10^{-11}$

**Table 6** Initial concentrations used for simulations of carene in the presence of ozone. Values used in simulations are in molecules  $\text{cm}^{-3}$ . Values in parentheses are mixing ratios (ppb) extracted from the literature.<sup>23</sup>

	$\Delta^3$ -Carene	Ozone
Test 1	$2.26 \times 10^{+12}$ (90.3)	$9.04 \times 10^{+12}$ (361)
Test 2	$3.58 \times 10^{+11}$ (15.1)	$1.42 \times 10^{+12}$ (60)
Test 3	$7.73 \times 10^{+11}$ (32.6)	$3.11 \times 10^{+12}$ (130)
Test 4	$1.20 \times 10^{+12}$ (50.0)	$4.79 \times 10^{+12}$ (200)

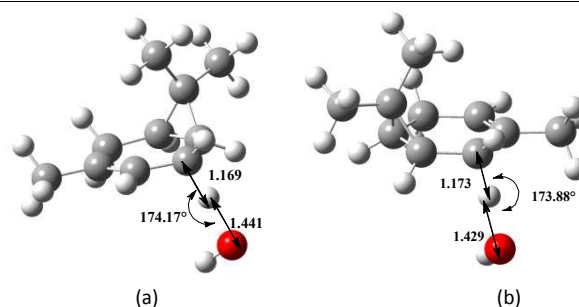


**Fig. 6** Transition structures optimised for the abstraction of allylic hydrogen of  $\Delta^3$ -carene at the BHandHLYP/6-311++G(d,p) level. Bond distances are given in angstroms and bond angles in degrees.

equation (5) and all of the rate coefficients of the abstraction channels. The rate coefficient including the abstraction and addition reactions,  $5.06 \times 10^{-12} \text{ cm}^3 \text{ molecule}^{-1} \text{ s}^{-1}$  at 298 K, is in better agreement with the experimental value and shows that, for this system, the contribution of the abstraction should not be neglected.

The integration of rate equations using the theoretical rate coefficients and all steps are illustrated in Figures 7 and 8†. For oxidation initialised by OH radicals, the addition and abstraction paths were included in the kinetic model. The atmospheric implication and other features will be discussed in the next section.

#### 40 Atmospheric Implications

Certain simplified numerical integration tests were performed using the rate coefficients calculated in the previous sections to check the major assumptions made in this study and to make predictions regarding  $\Delta^3$ -carene degradation in the presence of ozone and an OH radical. A complete mechanistic study will subsequently be performed using calculated or experimental rate coefficients for the further reactions of intermediate products with  $\text{O}_2$ , nitrogen oxides and other atmospheric oxidants to provide a complete description of  $\Delta^3$ -carene atmospheric oxidation and its impact on SOA formation.

The mechanism was simulated using a zero-dimensional model, the kinetic parameters determined in this study and the initial mixing ratios proposed by Colville and Griffin,<sup>23</sup> as shown in Table 6. The initial conditions used in the experiments and simulations for comparison<sup>23</sup> were higher than the values typically observed in the troposphere. In all simulations, the  $\Delta^3$ -carene concentration is halved before 300 min (5 hours, Figure 7), in agreement with the experiments and simulations reported by Griffin *et al.*,<sup>23,53</sup> who used  $\alpha$ -pinene data to develop their model. If typical atmospheric concentrations are considered—specifically,  $7 \times 10^{11} \text{ molecules cm}^{-3}$  for ozone<sup>18</sup> and a range of  $2.5 \times 10^9$  to  $1.5 \times 10^{10} \text{ molecules cm}^{-3}$  for  $\Delta^3$ -carene<sup>54</sup>—ozonolysis might be considered a pseudo-first-order reaction. Using the definition of lifetime as the time that a compound takes to decay to  $1/e$  from its initial concentration and the rate coefficient  $2.9 \times 10^{-17} \text{ cm}^3 \text{ molecule}^{-1} \text{ s}^{-1}$ , the theoretical expected lifetime for  $\Delta^3$ -carene in the presence of ozone is 19.1 hours. This value has been previously estimated by Atkinson and Arey,<sup>18</sup> for the same ozone concentration, to be 11 hours.

As expected, these simulations show that  $\Delta^3$ -carene is not readily

decomposed in the presence of ozone and that it remains in the atmosphere for 10 to 18 hours (considering different experimental results and the theoretical rate coefficient determined in this study).

In the simulations concerning OH radical addition, we used the concentration range proposed by Krasnoperov *et al.*<sup>55</sup> in their study of propene oxidation by OH radical:  $3.0 \times 10^{11}$ ,  $4.5 \times 10^{11}$  and  $6.0 \times 10^{11}$  molecules  $\text{cm}^{-3}$  for the OH radical. The  $\Delta^3$ -carene concentrations were the same as those used in the ozonolysis simulation. A range of lifetime values for  $\Delta^3$ -carene was obtained after the simulations because different combinations of  $\Delta^3$ -carene and OH concentrations were used. In most of the tests, the concentration of  $\Delta^3$ -carene is halved in less than  $2 \times 10^{-2}$  s, as expected because of the high reactivity of the OH radical (Figure 8). Throughout the simulation, the radical-dipole complexes have a concentration of nearly zero, in agreement with the assumption of a steady state for these species. Although four intermediate

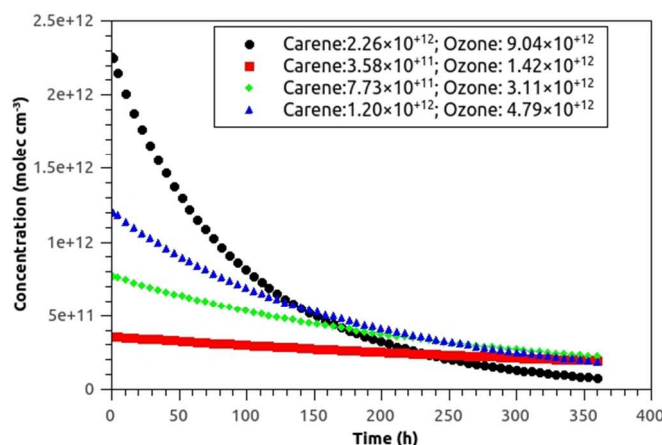


Fig. 7 Temporal behaviour of  $\Delta^3$ -carene in the presence of different ozone concentrations. Units in  $\text{cm}^3 \text{molecule}^{-1}$ .

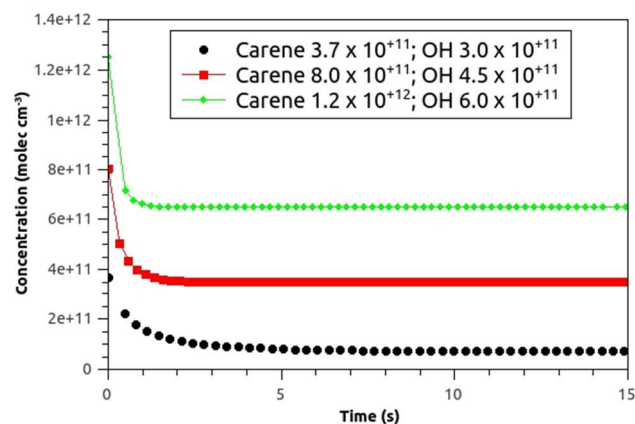


Fig. 8 Temporal behaviour of  $\Delta^3$ -carene in the presence of different concentrations of OH radical. Units in  $\text{cm}^3 \text{molecules}^{-1}$ .

species are expected, the addition on carbon 2 is more favourable than on carbon 1; consequently, the major oxidation products may be related to OH attack on carbon 2. This result differs from Colville's assumption<sup>23</sup> on the basis of similarities between  $\Delta^3$ -carene and  $\alpha$ -pinene,<sup>56</sup> where the OH radical adds to each center portion of the double bond at the same ratio (50%-50%). If the

abstraction reaction is considered, the second major channel is the hydrogen abstraction on carbon 3, followed by the abstraction on carbon 6 $\dagger$ .

In the atmosphere, the concentration of  $\Delta^3$ -carene is three orders of magnitude greater than that of OH radical. Considering an estimated diurnally, seasonally, and annually averaged overall OH concentration of approximately  $2 \times 10^6$  molecules  $\text{cm}^{-3}$ , the oxidation exhibits pseudo-first-order kinetics in OH radical, which provides a theoretical  $\Delta^3$ -carene lifetime time of approximately 3 min.

The overall lifetime ( $\tau_{\text{overall}}$ ) can be estimated using the following equation:<sup>57</sup>

$$\tau_{\text{overall}} = \left[ \frac{1}{\tau_{\text{Cl}}} + \frac{1}{\tau_{\text{OH}}} + \frac{1}{\tau_{\text{O}_3}} + \frac{1}{\tau_{\text{photolysis}}} + \frac{1}{\tau_{\text{others}}} \right]^{-1} \quad (6)$$

where  $\tau$  is the lifetime of  $\Delta^3$ -carene in the presence of each oxidant or in the presence of radiation.

In the conditions of this simulation, the  $\tau_{\text{overall}}$  in the presence of only ozone and OH radical was estimated to be approximately 3 min. In atmospheric conditions (OH and  $\text{O}_3$  mean concentrations of approximately  $2 \times 10^6$  and  $7 \times 10^{11}$  molecules  $\text{cm}^{-3}$ , respectively),  $\tau_{\text{overall}}$  can be estimated as 1.4 hours using the Atkinson and Arey data<sup>18</sup> and disregarding the  $\text{NO}_3$  reactions. In this study, this value was calculated to be 11.2 hours because of a slight underestimation of the rate constant. The exponential dependence of the rate coefficients on the activation parameters leads to a significant error in the kinetics properties. An error of 1  $\text{kJ mol}^{-1}$  in the free energy of activation leads to an error of 1 order of magnitude in the rate coefficient. This error has a dramatic impact on the estimated lifetimes. In fact, an error of a few units in the rate coefficients results in a difference of hours between the experimental and theoretical lifetimes. The inclusion of the abstraction path in the estimate of the overall rate coefficient for the reaction with OH radical modifies the lifetime by nearly 3 hours. These results show that the calculated rate coefficients should be improved to obtain reliable lifetimes. Further simulations should be performed that include the effects of other oxidants in the mechanism and those of competitive reactions and to analyse the ratio of products formed.

## Conclusions

The rate-limiting steps of  $\Delta^3$ -carene oxidation by  $\text{O}_3$  and OH radical were studied using quantum chemical methods. This study is, to the best of our knowledge, the first theoretical work to address the fundamental structural and energetic aspects of such reactions. The results show that the B3LYP functional is not adequate to describe these reactions. With respect to the ozonolysis reaction, a) the best agreement between theoretical and experimental rate coefficients was obtained using the TST theory and the energetic parameters evaluated at the CCSD(T)/6-31G(d,p)//PBE1PBE/6-311++G(d,p) level ( $2.08 \times 10^{-17}$   $\text{cm}^3 \text{molecules}^{-1} \text{s}^{-1}$ ); b) the addition in the bottom orientation is predominant because of its lower steric hindrance; c) the rate coefficient has a small temperature dependence and may be treated as constant for atmospheric modelling purposes; and d)  $\Delta^3$ -carene is expected to remain in the atmosphere between 10 and 18 hours in an atmosphere containing ozone as the unique

oxidant.

The evaluation of kinetic parameters for the addition of OH radical to the  $\Delta^3$ -carene double bond indicates that addition on carbon 2 is the major addition channel and that the abstraction reaction should not be neglected. The overall rate coefficient for this reaction was obtained by considering the formation and decomposition of two different radical-dipole complexes into four different adducts. The theoretical rate coefficient calculated at the BHandHLYP/6-311++G(d,p) level,  $5.06 \times 10^{-12} \text{ cm}^3 \text{ molecules}^{-1} \text{ s}^{-1}$ , is in reasonable agreement with the results of experimental measurements. For simulation purposes, the rate coefficients should be improved to provide better predictions of atmospheric conditions.

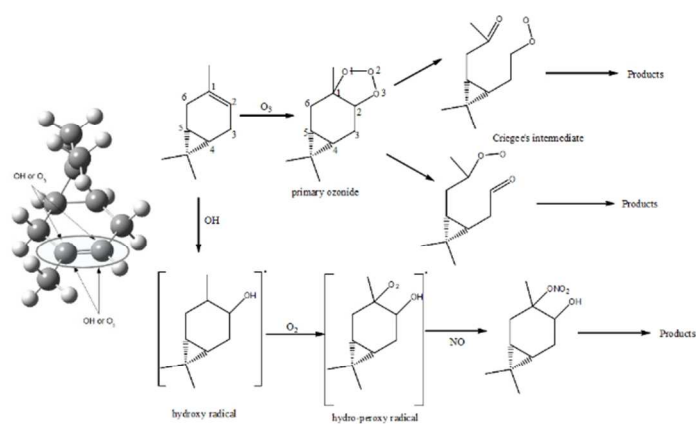
## 15 Acknowledgments

The authors thank CAPES, FAPERJ and CNPq for financial support and Professor Glaucio Favilla Bauerfeldt from Universidade Rural do Rio de Janeiro for helpful discussions.

## Notes and references

- <sup>20</sup> <sup>a</sup> Universidade do Estado do Rio de Janeiro, Faculdade de Tecnologia, Departamento de Química e Ambiental, Rodovia Presidente Dutra Km 298, Resende, RJ, Brazil Fax: +55 (24) 3381-3889; Tel: +55(24) 3381-3889; E-mail: leobap@gmail.com
- <sup>25</sup> <sup>b</sup> Universidade Federal do Rio de Janeiro, Instituto de Química, Departamento de Físico-Química, Macaé – RJ
- <sup>25</sup> <sup>c</sup> Universidade Federal do Rio de Janeiro, Instituto de Química, Departamento de Físico-Química, Ilha do Fundão – RJ
- † Electronic Supplementary Information (ESI) available: Kintecus graphics, thermochemistry and free energy profile for dissociation of pre-reactive complexes back to the separated reactants at 298 K. See DOI: 10.1039/b000000x/
- <sup>1</sup> G. P. Brausser, J.J. Orlando, G. S. Tyndall, *Atmospheric Chemistry and Global Change, New York: Oxford University Press, Inc.*, 1999.
- <sup>2</sup> T.M. Svendby, M. Lazaridis, K. Tørseth, *J. Atmos. Chem.*, 2008, **59**, 25
- <sup>3</sup> C. Alves, *Quim. Nova*, 2005, **28**, 859.
- <sup>4</sup> I.G. Kavouras, N. Mihalopoulos, E.G. Stephanou, *Environ.Sci. Technol.*, 1999, **33**, 1028.
- <sup>5</sup> B.J. Finlayson-Pitts, *Phys. Chem. Chem. Phys.*, 2009, **11**, 7760.
- <sup>6</sup> A. Presto, K. Huffhartz, N. Donahuen, *Environ. Sci. Technol.*, 2005, **39**, 7036
- <sup>7</sup> Y. Ma, A.T. Russell, G. Marston, *Phys. Chem. Chem. Phys.*, 2008, **10**, 4294
- <sup>8</sup> J. Yu, J., R.J. Griffin, D.R. Cocker, *et al*, *Geophys. Res. Lett.*, 1999, **26**, 1145
- <sup>9</sup> A. Aharoni, M. A. Jongsma, H. J. Bouwmeester, *Trends Plant Sci*, 2005, **10**, 1360
- <sup>10</sup> a) R. Atkinson, *J. Phys. Chem. Ref. Data*, 1997, **26**, 215; b) R. Griffin, D. Cocker, R. Flagan, J. Seinfeld, *J. Geophys. Res.*, 1999, **104**, 3555
- <sup>11</sup> a) R. Criegee, R., *Angew. Chem.*, 1975, **14**, 745; b) D. Johnson, G. Marston, *Chem. Soc. Rev.*, 2008, **37**, 699.
- <sup>12</sup> a) G. Marston, *Science*, 2012, **335**, 178; b) O. Welz, J.D. Savee, D. L. Osborn, S. S. Vasu, C. J. Percival, D. E. Shallcross, C. A. Taatjes, *Science*, 2012, **335**, 204.
- <sup>13</sup> C. A. Taatjes, D. E. Shallcross, C. J. Percival, *Phys. Chem. Chem. Phys.*, 2014, **16**, 1704
- <sup>14</sup> L. Vereecken, H. Harder, A. Novelli, *Phys. Chem. Chem. Phys.*, 2014, **16**, 4039
- <sup>15</sup> a) M.T. Nguyen, T.L. Nguyen, V.T. Ngan, H. M. T. Nguyen, *Chem. Phys. Lett.*, 2007, **448**, 183; b) I. Ljubic, A. Sabljic, *Chem. Phys.*, 2005, **309**, 157; c) D. Cremer, E. Kraka, P.G. Szalay, *Chem. Phys. Lett.*, 1998, **292**, 97.
- <sup>16</sup> T.L. Nguyen, J. Peeters, L. Vereecken, *Phys. Chem. Chem. Phys.*, 2009, **11**, 5643.
- <sup>17</sup> R. Atkinson, *Atmos. Environ.*, 2000, **34**, 2063
- <sup>18</sup> R. Atkinson, J. Arey, *Acc. Chem. Res.*, 1998, **31**, 574
- <sup>19</sup> A. Mellouki, G. Le Bras, H. Sidebottom, *Chem. Rev.*, 2003, **103**, 5077.
- <sup>20</sup> a) C.S. Gibson, J.L. Simonsen, *J. Chem. Soc.*, 1929, **January 1<sup>st</sup>**, 305; b) Holzke, C., T. Hoffmann, L. Jaeger, R. Koppmann, W. Zimmer, *Atmos. Environ.*, 2006, **40**, 3174.
- <sup>21</sup> a) Å. M. Jonsson, M. Hallquist, E. Ljungström, *Environ. Sci. Technol.*, 2005, **40**, 188; b) Å. M. Jonsson, M. Hallquist, E. Ljungström, *Environ. Sci. Technol.*, 2008, **42**, 5938
- <sup>22</sup> Y. Ma, R. A. Porter, D. Chappell, A. T. Russell, G. Marston, *Phys. Chem. Chem. Phys.*, 2009, **11**, 4184-4197
- <sup>23</sup> C. J. Colville, R. J. Griffin, *Atmos. Environ.*, 2004, **38**, 4001
- <sup>24</sup> M.E. Jenkin, S.M. Saunders, M.J. Pilling, *Atmos. Environ.*, 1997, **31**, 81
- <sup>25</sup> M. J. Frisch et. al. Gaussian 03, Revision B.04, Gaussian Inc., Pittsburgh PA, 2003.
- <sup>26</sup> F. Neese: The ORCA program system (WIRES Comput Mol Sci 2012, 2: 73-78.
- <sup>27</sup> J. C. Ianni, "A Comparison of the Bader-Deuflhard and the Cash-Karp Runge-Kutta Integrators for the GRI-MECH 3.0 Model Based on the Chemical Kinetics Code Kintecus", pg.1368-1372, Computational Fluid and Solid Mechanics 2003, K.J. Bathe editor, Elsevier Science Ltd., Oxford, UK., 2003
- <sup>28</sup> R. C. de M. Oliveira, G. F. Bauerfeldt, *J. Chem. Phys.*, 2012, **137**, 134306.
- <sup>29</sup> D. Zhang, R. Zhang, *J. Am. Chem. Soc.*, 2002, **124**, 2692
- <sup>30</sup> M. Olzmann, E. Kraka, D. Cremer, R. Gutbrod, S. Andersson, *J. Phys. Chem.*, 1997, **101**, 9421.
- <sup>31</sup> a) L. Baptista, R. Pfeifer, E. C. da Silva, Arbilla, *J. Phys. Chem. A*, 2011, **115**, 10911; b) T. Leonardo, G. Arbilla; E. C. da Silva, *J. Phys. Chem. A*, 2008, **112**, 6636.
- <sup>32</sup> a) R. Atkinson, D. Hasegawa, S. M. Aschmann, *Int. J. Chem. Kinet.*, 1990, **22**, 871; b) M. Witter, T. Berndt, O. Boge, F. Stratmann, J. Heintzenberg, *Int. J. Chem. Kinet.*, 2002, **34**, 394; c) E. P., Grimsrud, H. H. Westberg, R. A. Rasmussen, *Proc. Symp. Chem. Kinet. Data Upper Lower Atmos. 1974*, 1975, **0**, 183
- <sup>33</sup> L. A. Ripperton, H. E. Jeffries, O. White, *Adv. Chem. Ser.*, 1972, **113**, 219
- <sup>34</sup> E. P. Grimsrud, H. H. Westberg, R. A. Rasmussen, *Int. J. Chem. Kinet.* 1975, **1**, 183
- <sup>35</sup> R. Atkinson, A. M. Winer, J. N. Pitts, Jr., *Atmos. Environ.* 1982, **16**, 1017
- <sup>36</sup> F. Nolting, W. Behnke, C. Zetzsch, *J. Atmos. Chem.*, 1988, **6**, 47
- <sup>37</sup> V. G. Khamaganov, R. A. Hites, *J. Phys. Chem. A*, 2001, **105**, 815
- <sup>38</sup> D. Grosjean, E. L. Williams, E. Grosjean, J. M. Andino, J. H. Seinfeld, *Environ. Sci. Technol.*, 1993, **27**, 2754
- <sup>39</sup> D. Johnson, A. R. Rickard, C. D. McGill, G. Marston, *Phys. Chem. Chem. Phys.*, 2000, **2**, 323
- <sup>40</sup> R. Atkinson, R., S. M. Aschmann, J. Arey, *Atmos. Environ.*, 1990, **24**, 2647
- <sup>41</sup> T. L. Nguyen, R. Winterhalter, G. Moortgat, B. Kanawati, J. Peeters, L. Vereecken, *Phys. Chem. Chem. Phys.*, 2009, **11**, 4173
- <sup>42</sup> L. Vereecken, J. S. Francisco, *Chem. Soc. Rev.*, 2012, **41**, 6259
- <sup>43</sup> R. Atkinson, *Chem Rev.*, 1985, **85**, 69.

- <sup>44</sup> J. J. Orlando, G. S. Tyndall, N. Ceazan, *J. Phys. Chem. A*, 2001, **105**, 3564
- <sup>45</sup> J. Peeters, W. Boullart, V. Pultau, S. Vandenberg, L. Vereecken, *J. Phys. Chem. A*, 2007, **111**, 1618
- <sup>46</sup> J. Peeters, S. Vandenberg, E. Piessens, V. Pultau, *Chemosphere* 1999, **6**, 1189
- <sup>47</sup> J. E. Ham, S. P. Proper, J.R. Wells, *Atmos. Environ.*, 2006, **40**, 726
- <sup>48</sup> C. D. Forester, J.R. Wells, *Environ. Sci. Technol.* 2009, **43**, 3561
- <sup>49</sup> R. Atkinson, *J. Phys. Chem. Ref. Data, Monograph 1*, 1989, 246.
- <sup>50</sup> A. Montenegro, J. S. A. Ishibashi, P. Lam, Z. Li, *J. Phys. Chem. A*, 2012, **116**, 12096
- <sup>51</sup> a) L. Baptista, E. C. da Silva, G. Arbilla, *J. Mol. Struct.: THEOCHEM*, 2008, **851**, 1; b) A. Galano, J. R. Alvarez-Idaboy, G. Bravo-Pérez, Ma. E. Ruiz-Santoyo, *Phys. Chem. Chem. Phys.*, 2002, **4**, 4648, c) N. González-García, A. González-Lafont, J. M. Lluch, *J. Phys. Chem. A*, 2006, **110**, 798
- <sup>52</sup> a) R. Atkinson, S. M. Aschmann, J.N Pitts Jr., *Int. J. Chem. Kinet.*, 1986, **18**, 287; b) J. Peeters, W. Boullart, V. Pultau, S. Vandenberg, L. Vereecken, *Phys. Chem. A*, 2007, **111**, 1618; c) D. Grosjean, E.L. Williams II, *Atmos. Environ. Part A*, 1992, **26**, 1395
- <sup>53</sup> R.J. Griffin, D.R Cocker III, R.C. Flagan, J.H Seinfeld, J.H., *J. Geophys. Res.*, 1999, **104**, 3555
- <sup>54</sup> G. W. Shade, A. H. Goldstein, M. S. Lamanna, *J. Geophys. Res. Let.*, 1999, **26**, 2187
- <sup>55</sup> L. N. Krasnoperov, N. Butkovskaya, G. Le Bras, *J. Phys. Chem. A*, 2011, **115**, 2498
- <sup>56</sup> J. Peeters, L. Vereecken, G. Fantechi, *Phys. Chem. Chem. Phys.*, 2001, **3**, 5489
- <sup>57</sup> J. H. Seinfeld, S. N. Pandis, *Atmospheric Chemistry and Physics - From Air Pollution to Climate Change*, 2<sup>nd</sup> ed, John Wiley & Sons



The rate-limiting steps of  $\Delta$ -3-(+)-carene oxidation by ozone and OH were studied by quantum-chemical methods and the atmospheric implications discussed.